TOR represses stress responses through global regulation of H3K27 trimethylation in plants

Yihan Dong[1, 3, @], Veli V. Uslu[2, 3, @], Alexandre Berr[1], Gaurav Singh[1], Csaba Papdi[1], Victor A Steffens[2], Thierry Heitz[1] and Lyubov Ryabova[1, @]

1. Institute de Biologie Moléculaire des Plantes, Centre National de la Recherche Scientifique, UPR 2357, Université de Strasbourg, Strasbourg, France.
2. AgroScience GmbH, Neustadt an der Weinstraße, 67435, Germany.
3. These authors contributed equally.

[@]Corresponding authors:

yihan.dong@ibmp-cnrs.unistra.fr

velivural.uslu@agroscience.rlp.de

lyuba.ryabova@ibmp-cnrs.unistra.fr

Key words: Target of Rapamycin, H3K27me3, H3K4me3, bistable chromatin, CLF, LHP1, BRM, Stress response, biotic stress.

Abstract

Target of Rapamycin (TOR) functions as a central sensory hub to link a wide range of external stimuli to gene expression. However, the mechanisms underlying stimulus-specific transcriptional reprogramming by TOR remains elusive. Our *in silico* analysis in Arabidopsis demonstrates that TOR-repressed genes are associated with either bistable or silent chromatin states. Both states regulated by TOR signaling pathway are associated with high level of H3K27me3 deposited by CURLY LEAF (CLF) in specific context with LIKE HETEROCHROMATIN PROTEIN1 (LHP1). Combinations of epigenetic modifications H3K4me3 and H3K27me3 implicate bistable feature which alternates between on and off state allowing rapid transcriptional changes upon external stimuli. Chromatin remodeler SWI2/SNF2 ATPase BRAHMA (BRM) activates TOR-repressed genes only at bistable chromatin domains to rapidly induce biotic stress responses. Here we demonstrated both *in silico* and *in vivo* that TOR represses transcriptional stress responses through global maintenance of H3K27me3.

35 **Introduction**

36 The protein kinase TOR is a conserved sensor of nutrient availability and energy status in
37 eukaryotes, known to regulate many fundamental cellular processes, such as translation,
38 autophagy and cell cycle (1). In animals, since diet and nutrient exert transgenerational
39 effect, correlations between TOR functions and epigenome started to be explored (2).
40 Besides the known relationship between histone acetylation and mammalian TOR (mTOR)
41 signaling pathway, mammalian/mechanistic TOR complex 1 (mTORC1) was recently found to
42 activate its canonical substrate S6K1 which in turn phosphorylates histone H2B to influence
43 histone methylation(2). Unlike in animals, little is known in plants to link TOR function to
44 epigenetic modifications.

45

46 As sessile organisms, plants continuously and rapidly adjust their development to a
47 multitude of environmental stresses. Beyond stress sensing and signal transduction, plant
48 TOR tunes developmental plasticity via its capacity to re-program the transcriptome (3). This
49 global transcriptional reprogramming is partially mediated by the retention of ethylene-
50 insensitive protein 2 (EIN2) in the cytoplasm to allow gene expression involved in DNA
51 replication and cell wall biosynthesis (4). However, it still remains obscure how an active TOR
52 can suppress stress response and defense mechanism at transcriptional level. Among other
53 mechanisms, epigenetic modifications such as DNA methylation and histone modifications
54 have emerged as fundamental mediators in controlling gene expression.

55

56 Multiple combinations of different epigenetic modifications exist at the whole genome level
57 and contribute to the complexity of epigenetic landscapes. By reducing their dimensionality,
58 a detailed bioinformatic integration of epigenomic data defines distinctive chromatin states

59 (CS) in *A. thaliana* (5). The two silent states CS-8 and 9 are enriched in H3K9me2 and
60 H3K27me1 and preferentially mark constitutive heterochromatin. Another inactive state CS-
61 5 represents the typical Polycomb-regulated facultative heterochromatin with abundant
62 H3K27me3. Meanwhile, CS-1, 3 and 6 are characterized by high amounts of active marks
63 (*e.g.*, H3K4me3, H3 acetylation, H3K36me3) and typically found at actively transcribed genes.
64 Despite their opposite effect on transcription, H3K4me3 and H3K27me3 can co-reside at a
65 number of dynamically regulated genes in both animals and plants. This feature is the
66 hallmark of CS-2, a state preferentially found at the promoter of genes with transcript
67 amounts similar to the ones marked by CS-5. A bistable model of regulation achieved
68 through the delicate balance between H3K4me3 and H3K27me3 was proposed to poise
69 silenced genes marked by CS-2 for rapid activation upon need (6, 7). Adding additional layers
70 of complexity, chromatin-binding proteins like H3K27me3 reader LIKE HETEROCHROMATIN
71 PROTEIN 1 (LHP1) or SWI2/SNF2 ATPase BRAHMA (BRM) further subdivide these chromatin
72 domains into distinct subdomains (8-10).
73
74 In this study, we show that specific epigenetic features represent a dynamic hallmark of
75 stimulus-specific transcriptional responses mediated by TOR signaling upon environmental
76 stimuli. We demonstrate that active TOR represses genes associated with bistable (CS2) or
77 silent chromatin domains (CS5) by mediating the deposition of H3K27me^3 via CLF and LHP1.
78 We propose a model in which environmental stimuli inhibit TOR, which subsequently allows
79 BRM to reduce repression of bistable domains to rapidly activate biotic stress specific gene
80 expression.
81

82 **Results**

83 TOR-repressed genes are associated with CS-2 and CS-5 at the transcription
84 start site

85 To assess whether specific functional categories are enriched in any of the previously
86 described chromatin states, we performed gene ontology (GO) enrichment analysis (5).
87 Arabidopsis genes were individually assigned to one of the nine chromatin states based on
88 the chromatin state present at their TSS. Surprisingly, each of the nine chromatin states
89 were enriched in distinct functional categories (Fig. 1A and Table S1). Indeed, genes related
90 to protein and RNA processes appeared highly enriched in CS-1, 3 and 6, which are
91 characterized by the presence of active epigenetic marks. The Polycomb-associated CS-5
92 contained significantly more transcription, cell differentiation, and redox-regulation related
93 genes. Abiotic and biotic stress genes are overrepresented in the bistable CS-2.Worth noting,
94 functional categories enriched in CS-2 resemble the primary target genes in stress and
95 immune response pathways repressed by TOR (11). Because of this similarity, we next
96 search for particular chromatin state enrichments among TOR repressed genes.

97

98 A list of genes up-regulated (fold change>2.0; $p<0.05$) upon TOR inhibition by AZD8055
99 (AZDup, 1583 genes) or RNA interference (TOR-RNAi, 369 genes) was extracted from
100 published datasets (11, 12). 233 genes upregulated in both conditions were significantly
101 enriched at their TSS in the bistable CS-2 and also in the canonical Polycomb CS-5 (Fig. 1B).
102 These findings suggest that the repression of gene expression by TOR is achieved through
103 either CS-2 or CS-5. Furthermore, by distinguishing up-regulated genes depending on their
104 fold change, we observed that the CS-5 enrichment gradually increases with the fold change,
105 which is also the case for CS-2 but not beyond 16-fold change. In addition, more than half of

106 the CS-2 genes change only 2-4-fold (Fig. 1C and Fig. S1). This striking difference could reflect
107 the bistability of CS-2, in which frequent switches between active and silent state may occur,
108 resulting in a low rate of basal transcription, while TOR-repressed genes marked by the
109 monostable silent CS-5 are completely repressed.
110
111 Next, using GO analysis, we tested whether AZDup genes marked by either CS-2 or CS-5 are
112 enriched in particular functional categories. AZDup genes marked by CS-2 are enriched in
113 biotic stress and defense mechanisms mediated by phytohormone signaling (Fig. 1D, E),
114 whereas, abiotic stress related genes involved in oxidative stress and hypoxia response are
115 more abundant among AZDup genes with CS-5 features (Fig. 1F). This dichotomy indicates a
116 chromatin state dependent functionalization of TOR repressed genes.
117

118 The chromatin context of TOR-responsive genes is coordinately repressed by 119 CLF and LHP1

120 Based on the preferential association between TOR repressed genes and CS-2/5, both
121 characterized by the presence of H3K27me3, we hypothesized that a functional link may
122 exist between chromatin factors involved in H3K27me3 deposition and TOR. We tested this
123 hypothesis by collating the TOR repressed gene set with transcript profiles of Polycomb
124 mutants. CURLY LEAF (CLF), a Polycomb group (PcG) protein, is a major H3K27 tri-methylase
125 in plants (13). A total of 84 genes are shared between AZDup and those genes upregulated in
126 the loss-of-function *clf28* and *clf29* mutants (Fig. 2A). These shared genes display a
127 significantly higher association with CS-2 (OR=3.86) at their TSS than the AZDup or the up-
128 regulated genes in either *clf28* or *clf29* (Fig. 2B and Fig. S2). Reinforcing this positive
129 association, the CS-2 enrichment of AZDup decreases when the genes up-regulated in *clf*

130 mutants are excluded (AZDno*clf28/29*; Fig. 2B). Similarly, the CS-5 enrichment is remarkably
131 higher for genes upregulated in both AZDup and *clf* mutants compared to the genes
132 upregulated only in AZDup (AZDno*clf28*/29; Fig. 2B and Fig. S2). Furthermore, the GO
133 analysis of the 84 commonly up-regulated genes between AZDup and *clf* mutants points
134 toward a chromatin state dependent functional categorization. Indeed, commonly up-
135 regulated genes within CS-2 are significantly enriched in biotic and abiotic stress responses,
136 while the ones within CS-5 are specifically enriched in redox processes (Fig. 2C). Then we
137 tested the resistance of the *clf29* mutant to the TOR inhibitor AZD8055. Compared to the
138 wild-type control, *clf29* mutants did not respond to AZD8055 (Fig. 2D), which suggests that
139 growth arrest by TOR inactivation is largely dependent on loss of H3K27me3.
140
141 PcGs are generally classified into two major complexes named Polycomb Repressive
142 Complexes (PRC1 and PRC2) and CLF, a major PCR2 subunit, selectively collaborates with
143 different PcGs partners to achieve gene repression in distinct developmental programs (14).
144 A first group represents genes commonly up-regulated in *clf* and *lhp1* mutants and may
145 correspond to direct targets of CLF and LHP1 (*i.e.,* here after named CLF-LHP1-dependent
146 genes). The second one refers to genes more specifically affected in PRC1 mutants (*i.e.,* here
147 after named PRC1-PRC2 dependent genes). Thus, to dissect the relationship between TOR
148 and CLF transcriptional repression, we tested overlaps between these two groups and
149 AZDup genes. A significant overlap was observed between AZDup and CLF-LHP1-dependent
150 genes, while it was not the case with PRC1-PRC2 dependent genes (Fig. 2E). This result
151 suggests that CLF and LHP1 may work concertedly to participate in the repression of TOR
152 specific target genes.
153

154 We further investigated the link between TOR and LHP1 by focusing on the 111 genes
155 commonly upregulated by AZD8055 and in the *lhp1* mutant (Fig. 2F). In a manner similar to
156 genes co-upregulated by AZD and *in clf mutants*, these genes showed a significant
157 enrichment in both CS-2 and CS-5 (Fig. 2G and Fig. S3). When we analyzed overlap between
158 LHP1-target genes and genes up-regulated by AZD8055, we found that 445 out of 1583
159 AZDup genes are indeed targeted by LHP1 (Fig. S4A). CS-2 enrichment of AZDup genes was
160 decreased when LHP1 targets were excluded, whereas genes both upregulated by AZD and
161 targeted by LHP1 present an increased CS-2 enrichment compared to genes *sole* upregulated
162 by AZD or targeted by LHP1 (Fig. S4B). In addition, we noted that the LHP1 targeting also
163 increase the CS-5 enrichment of AZDup genes (Fig. S4B). This observation is reinforced by
164 the fact that when LHP1 direct targets were excluded the association between AZDup and
165 CS-5 dropped dramatically (Fig. S4B). Finally, we investigated whether LHP1 targeting
166 specifies TOR functions using GO analysis. The functional annotation obtained with the CS-2
167 subset of AZDup genes targeted by LHP1 is mainly linked to biotic and abiotic stress-related
168 functions (Fig. S4C). On the other hand, the functional annotations obtained with the CS-5
169 subset of AZDup genes targeted by LHP1 appears mainly related to oxidative stress and
170 hypoxia responses (Fig S4D). Together, our results indicate that besides being regulated
171 jointly by CLF and LHP1, TOR repressed targets may further split in distinct functional
172 categories depending on their respective CS-2 or CS-5 chromatin context.
173

174 BRM is important for activating genes associated with CS-2, when TOR is down-
175 regulated in response to biotic stress

176 TrxG proteins are evolutionarily conserved chromatin-modifying factors that antagonize PcG
177 repression and interactions between PcG/TrxG support a molecular basis for chromatin

178 bistability (7, 15). Among TrxG proteins, the SWItch/Sucrose Non-Fermentable (SWI/SNF)-
179 type protein BRAHMA (BRM) restricts CLF occupancy/activity at many developmental genes
180 (16). We therefore wondered whether the TrxG protein BRM would participate in
181 establishing bistable chromatin at the CS-2 subset of TOR regulated genes. Considering BRM
182 as an activator of gene expression, we observed a significant overlap between AZDup genes
183 and genes down-regulated in *brm1* mutant (Fig. S5) and also found that 57% of AZDup genes
184 are BRM targets (Fig. 3A). Moreover, the CS-2 enrichment among BRM targets was further
185 reinforced when including the overlap with AZDup (Fig. 3B and Fig. S6). Then, our GO
186 analysis demonstrates that AZDup genes which overlap with BRM target genes are mostly
187 biotic stress related, while BRM targets not suppressed by TOR are mostly related to
188 transcriptional regulation (Fig. 3C).
189
190 While keeping in mind the bistability of CS-2, we analyzed the overlap between the TrxG
191 component BRM targets and the PcG component LHP1 targets. A total of 1216 genes are co-
192 targeted by BRM and LHP1, among which 240 genes appeared as AZDup (Fig. S7A). Further
193 reinforcing a functional link between TOR repressed genes and bistable chromatin, these
194 genes show the highest CS-2 enrichment in this study. Furthermore, this result suggests that
195 BRM and LHP1 together act on TOR repressed genes to establish chromatin bistability (Fig.
196 S7B, C). Our GO analysis reveals a preferential enrichment in biotic stress related terms for
197 the CS-2 category, while the Cs-5 was preferentially enriched in GO terms related to
198 oxidative stress and hypoxia. This observation suggests a functional dichotomy between
199 AZDup genes co-targeted by BRM and LHP1 in CS-2 and AZDup genes targeted by LHP1 in CS-
200 5. Notably, the 976 genes co-targeted by BRM and LHP1 but not upregulated upon TOR
201 inhibition preferentially belong to TOR-independent functional categories, *e.g.*, salinity

202 response, auxin and gibberellin signaling at CS2; transcription regulation and cell wall
203 modification at CS-5 (Fig. S8).
204
205 The proposed functional dichotomy among TOR repressed genes implies that, within CS-2,
206 BRM may specifically activate genes involved in defense mechanism upon TOR inhibition by
207 a biotic stress signal. In agreement, it has been previously shown that over-expression of
208 TOR increased the susceptibility to both bacterial and fungal infections (17). To explore in
209 more details the role of BRM in regulating biotic stress related genes within CS-2, *brm5*
210 mutants were inoculated with the fungal pathogen *Botrytis cinerea*. Compared to the wild-
211 type control (Col-0), *brm5* mutants exhibited an enhanced susceptibility to *B. cinerea* with a
212 significant increase in lesion size while *clf29* did not (Figs 3D, E). Supporting our *in-silico*
213 analyses, opposite sensitivities were observed when mutants were tested for their response
214 to hypoxia caused by submergence. Indeed, while *brm5* behaved similarly as Col0, *clf29*
215 mutants were significantly less resistant to submergence (Figs 3F, G). Together, our results
216 indicate that BRM contributes to the functional specification of TOR responding genes.
217

218 TOR coordinates global H3K27me3 level at different growth and developmental 219 stages

220 The different correlations highlight a functional link between TOR and H3K27me3
221 transcriptional repression. We therefore hypothesize that the activation of TOR repressed
222 targets associated with CS-2 and CS-5 may require an active removal of H3K27me3. To test
223 this hypothesis, Arabidopsis were treated for 24 hours with AZD8055 to inhibit TOR.
224 Interestingly, AZD8055 treatment provoked a decrease in the global level of H3K27me3 (Fig.
225 4A). In a complementary approach, we also explore the impact of a TOR inhibition on the

226 global level of H3K27me3 by means of quantitative immuno-staining on root nuclei. In
227 agreement with the pharmaceutical inhibition of TOR by AZD8055, the level of fluorescence
228 intensity of H3K27me3 was significantly decreased upon inhibition of TOR by estradiol-
229 inducible TOR RNAi with fluorescence levels were intermediate between those of the mock-
230 treated control and the *clf29* mutant (Fig. 4B).
231
232 Both TOR kinase and H3K27me3 are important for photomorphogenesis. In the darkness,
233 TOR activity is repressed by COP1 to allow skotomorphogenesis *(18)*. Upon light exposure,
234 genome-wide profiling of H3K27me3 identified a gain in H3K27me3 for more than 2000
235 genes *(19)*. To gain more biological insight, we further tested whether H3K27me3 level is
236 correlated with TOR activity during photomorphogenesis. In agreement with published data
237 (18), light-grown seedlings, synonymous of TOR stimulation, had higher H3K27me3 than
238 dark-grown etiolated seedlings. Similarly, glucose, as a potent TOR activator (3), also
239 provoked an increase in H3K27me3. In the *cop1* mutant where TOR is pre-induced even in
240 the dark (19), H3K27me3 level was also maintained high to allow photomorphogenesis (Fig.
241 4C). Together, we conclude that TOR can recruit histone-modifying complexes including
242 CLF/LHP1 to promote H3K27 tri-methylation thus ultimately leading to the transcriptome
243 regulation.
244

245 **Discussion**

246 In plants, increasing evidence supports that TOR functions as a rheostat to fine-tune the
247 balance between growth and defense (17). However, molecular mechanisms responsible for
248 this balancing operation are still unclear and based on sparse information. Here, we propose
249 a bipartite model in which TOR acts upstream to repress two separate sets of stress related
250 genes by means of two distinct chromatin contexts: *i*) the bistable CS-2 for genes involved in
251 fine-tuning specific stress responses and *ii*) the repressive CS-5 for more general and non-
252 specific stress related genes involved in redox processes and hypoxia responses (Fig. 4D). In
253 agreement with the global effect of TOR inhibition on H3K27me3, we noticed a significant
254 enrichment of CS-2 and CS-5 (*i.e.*, two chromatin state characterized notably by the
255 presence of the repressive histone mark H3K27me3) at TOR repressed genes. In addition, we
256 identified significant correlations between TOR-regulated genes and several chromatin
257 factors. LHP1, a plant-specific polycomb subunit, works concertedly with CLF to deposit and
258 spread H3K27me3 and contributes to specify CLF collaborations with different PcGs partners
259 to achieve transcriptional repression in distinct developmental programs (14).

260

261 Despite the enrichment in both CS-2 and CS-5 detected among genes up-regulated in *CLF*
262 and *LHP1* loss-of-function mutants, CLF and LHP1 targets were under-represented in CS-2
263 but preferentially enriched in CS-5 (Fig. S4B and Fig. S9A). In a similar manner, while being
264 significantly enriched in CS-2, genes up-regulated upon TOR inhibition were under-targeted
265 by CLF (Fig. S9B). Considering the bistable nature of CS-2, we believe that these
266 discrepancies may reflect a too transient/dynamic to be captured binding of CLF-LHP1 on CS-
267 2 genes, a labile mechanism proposed as the basis for chromatin bistability (20). Also, these
268 CS-2 genes are not expressed under normal growth conditions due to the presence of

269 H3K27me3. However, H3K4me3 poises them to quickly switch from silent to active
270 transcriptional states in response to TOR inactivation. Such chromatin context may
271 contribute to facilitate a rapid transcriptional response to stress, thus providing an enhanced
272 protection without the costs incurred from the constitutive expression of stress related
273 genes. The coordinate action of CLF and LHP1 seems also to be involved in the deposition of
274 H3K27me3 at CS-5 genes repressed by TOR. CS-2 and CS-5 genes were enriched in distinct
275 functional categories, with CS-5 significantly enriched in genes related to oxidative stress.
276 Interestingly, oxidative stress occurs in response to any kind of environmental cues and
277 antioxidant processes has been proposed to improve the tolerance of plants to various
278 stresses (21). Therefore, the distinctly enriched functional categories we found may reflect
279 different processes of gene expression engagement with CS-2 prevailing for stress response
280 genes and CS-5 for stress tolerance genes.
281
282 In an antagonistic manner to CLF-LHP1, we also proposed that the TrxG protein BRM may
283 contribute to regulate CS-2 genes repressed by TOR. This antagonism may occur through its
284 known partner, the H3K27 demethylase REF6 (22). Interestingly, BRM was previously
285 positioned at the nexus of the resource allocation decision between growth and stress
286 responses (23), a positioning which dovetails TOR functions in balancing plant growth and
287 stress responses in response to environmental cues. In addition, BRM is a phosphorylation
288 target of the ABA-SnRK2 relay, which reciprocally regulates the TOR signaling pathway (24,
289 25). Moreover, BRM protein sequence contains several TOR phosphorylation consensus sites,
290 suggesting that the distinct phosphorylation of BRM by TOR and/or SnRK2 may specify its
291 function (26).
292

293 Besides BRM, TOR may regulate H3K27me3 through controlling mRNA translation of several
294 enzymes involved in H3K27 methylation and/or demethylation. La-related protein 1 (LARP1)
295 is a RNA binding protein conserved across eukaryotes and involved in regulating 5' terminal
296 oligopyrimidine motif (5'TOP) mRNA translation. Recent studies have shown that TOR
297 phosphorylates LARP1 in plants, thus regulating the translation efficiency of 5'TOP-mRNAs
298 that possibly encode proteins involved in chromatin remodeling, e.g. LHP1 (26, 27). In
299 addition, TOR may also regulate the availability of a particular methylation substrate, such as
300 the universal methyl donor S-adenosyl-methionine (SAM) that functions in the methionine-
301 folate cycle. Interestingly, MTHFD1 is a folate cycle enzyme impacting global DNA
302 methylation in plants through SAM availability (28). In animals, mTORC1 senses SAM levels
303 through SAMTOR and MTHFD transcription under tight control of mTORC1 (29, 30). However,
304 it remains unknown whether plant TOR modulates DNA or histone methylation through SAM
305 metabolism in plants. SAMTOR seems to be also a metazoan invention.
306
307 In both animals and plants, TOR function is primarily linked to nutrient sensing and
308 translational control. Our findings reveal a novel regulatory role of TOR signaling in
309 chromatin remodeling to modulate specific transcriptional responses. We have identified
310 multiple players involved in this regulation, but additional components are yet to be
311 discovered. In the future, it will be of great importance to dissect this new signaling
312 pathway to understand the role of TOR-dependent epigenetic reprogramming in
313 environmental responses at transitions of developmental stages.
314

315 **Methods**

316 Plant materials and growth condition

317 *Arabidopsis thaliana* mutant plants, as well as wild-type control plants were the Columbia
318 (Col-0) ecotype. Wild-type plants (N1092) and *brm-5* (N68980) were gained from the
319 European Arabidopsis Stock Centre. *clf-29* (SALK_021003) mutant was described in Wang et
320 al., 2016 (14). *cop1-4* was described in (19). ß-estradiol inducible TOR-RNAi line was
321 described in (3). All seedlings were grown on 1/2MS medium (pH5.7, 0.8% agar) in a long-
322 day climate chamber (16 h light/8 h dark; 80-100 µmol m-2s-1; 22°C day/18°C night; 50%
323 humidity). Chemical inhibitor treatments were performed with media containing 0.2 µM
324 AZD-8055 for 10 days or 1 µM for 24 hours. Submergence was performed with 5 week soil-
325 grown plants for 24 hours and recovered for 1 week in the short-day climate chamber (12 h
326 light/12 h dark).

327

328 Western blot

329 For immunological detection, total soluble proteins were extracted from 50 mg plant
330 materials with 250 µl 2x Laemmli buffer. Proteins were denatured for 5 min at 95°C and
331 separated on 15% SDS-PAGE. Subsequently, proteins were blotted to PVDF membrane. The
332 primary antibodies anti-H3K27me3 (1:5000, Agrisera, AS16-3193) and anti-H3 (1:5000,
333 Agrisera, AS10-710) were detected using the HRP-conjugated secondary antibody (1:20,000).
334 Full western blot images are provided in Fig. S10.

335

336 Fungi infection

337 *B. cinerea* was inoculated on 5-week-old soil-grown plants in a short-day chamber (12 h
338 light/12 h dark; 80-100 µmol m-2s-1; 22°C day/18°C night; 50% humidity). For the lesion

339 assay, 5-µL droplets of *B. cinerea* spore suspension were placed directly on the upper surface
340 of the leaf. After inoculation, plants were kept with full humidity to facilitate the infection.
341 Lesions were measured 3 days after the inoculation.
342

343 Chromatin state enrichment analysis

344 Chromatin states were defined based on Hidden Markov Model (HMM) and previously
345 defined coordinates were extracted (Sequeira-Mendez et al., 2014). The gene sets are given
346 in Supplementary file. Transcription start sites (TSS) and transcription termination sites (TTS)
347 are downloaded from www.arabidopsis.org (TAIR10). An array is formed for each region of
348 interest. GenomicRanges R-package was used to match the genes in each set with a
349 chromatin state (31). The enrichment of chromatin states were calculated by odd ratio (OR)
350 and False Discovery Rate (FDR) adjusted p values were used to define the significance of OR.
351 Statistical comparison of different ORs were performed by Fisher's exact test and statistical
352 significance threshold is taken as $p<0.05$. All the gene lists extracted from published datasets
353 and analyzed in this work are provided in Supplementary file.
354

355 Immunostaining and microscopy

356 Immunostaining was performed as described previously (32) on 7-days-old *in-vitro* grown
357 seedlings of Col-0, TOR-RNAi and *clf-29* treated or not for 24h with 10 µM ß-estradiol.
358 Antibodies used for immunostaining were the anti-H3K27me3 (1:500) and the Alexa fluor-
359 488 dyes-conjugated secondary antibody (1:1000, Life Technologies, A-11008). The
360 H3K27me3 signal intensity for each nucleus was calculated relative to the intensity of DAPI
361 using ImageJ software. Confocal images were acquired with a Zeiss LSM-700 microscope
362 with a 63x/1.01 objective.

363

364 ## Acknowledgement

365 We thank D. Janocha (University of Heidelberg) for providing *cop1* mutants, French Agence
366 Nationale de la Recherche— ANR-18-CE13-0019 – ReinitiaTOR to L.R. and 2020 Marie Curie
367 fellowship 885864 TOR in acTIon MSCA-IF-EF-ST to Y.D.

368

369 ## Author contribution

370 Y.D. and V.U.U. initiated the project. Y.D., V.U.U., A.B. and C.P. contributed to experiment
371 design and project development. Y.D. coordinated the project and performed experiments.
372 V.U.U. and V.A.S performed bioinformatic analysis. A.B. and G.S. performed immuno-
373 staining. Y.D. and T.H. performed *B. cinerea* infection. Y.D., V.U.U. and A.B. made figures and
374 wrote the manuscript. C.P., T.H. and L.R. revised the manuscript.

375

376 ## Declaration of interest

377 The authors declare that the research was conducted in the absence of any commercial or
378 financial relationships that could result in any potential conflict of interest.

379

380 ## Data availability

381 All datasets generated for this study are included in the manuscript and/or the
382 Supplementary Files.

383

384 **References**

385 1. Saxton RA & Sabatini DM (2017) mTOR Signaling in Growth, Metabolism, and Disease.
386 *Cell* 169(2):361-371.
387 2. Laribee RN & Weisman R (2020) Nuclear Functions of TOR: Impact on Transcription
388 and the Epigenome. *Genes (Basel)* 11(6).
389 3. Xiong Y*, et al.* (2013) Glucose-TOR signalling reprograms the transcriptome and
390 activates meristems. *Nature* 496(7444):181-186.
391 4. Fu L*, et al.* (2021) The TOR-EIN2 axis mediates nuclear signalling to modulate plant
392 growth. *Nature*.
393 5. Sequeira-Mendes J*, et al.* (2014) The Functional Topography of the Arabidopsis
394 Genome Is Organized in a Reduced Number of Linear Motifs of Chromatin States.
395 *Plant Cell* 26(6):2351-2366.
396 6. Schwartz YB*, et al.* (2010) Alternative epigenetic chromatin states of polycomb target
397 genes. *PLoS Genet* 6(1):e1000805.
398 7. Sneppen K & Ringrose L (2019) Theoretical analysis of Polycomb-Trithorax systems
399 predicts that poised chromatin is bistable and not bivalent. *Nat Commun* 10(1):2133.
400 8. Torres ES & Deal RB (2019) The histone variant H2A.Z and chromatin remodeler
401 BRAHMA act coordinately and antagonistically to regulate transcription and
402 nucleosome dynamics in Arabidopsis. *Plant J* 99(1):144-162.
403 9. Gomez-Zambrano A, Merini W, & Calonje M (2019) The repressive role of Arabidopsis
404 H2A.Z in transcriptional regulation depends on AtBMI1 activity. *Nat Commun*
405 10(1):2828.
406 10. Liu Y*, et al.* (2018) PCSD: a plant chromatin state database. *Nucleic Acids Res*
407 46(D1):D1157-D1167.
408 11. Dong P*, et al.* (2015) Expression profiling and functional analysis reveals that TOR is a
409 key player in regulating photosynthesis and phytohormone signaling pathways in
410 Arabidopsis. *Frontiers in Plant Science* 6.
411 12. Caldana C*, et al.* (2013) Systemic analysis of inducible target of rapamycin mutants
412 reveal a general metabolic switch controlling growth in Arabidopsis thaliana. *The*
413 *Plant Journal* 73(6):897-909.
414 13. Mozgova I & Hennig L (2015) The polycomb group protein regulatory network. *Annu*
415 *Rev Plant Biol* 66:269-296.
416 14. Wang H*, et al.* (2016) Arabidopsis Flower and Embryo Developmental Genes are
417 Repressed in Seedlings by Different Combinations of Polycomb Group Proteins in
418 Association with Distinct Sets of Cis-regulatory Elements. *PLoS Genet* 12(1):e1005771.
419 15. Ringrose L (2017) Noncoding RNAs in Polycomb and Trithorax Regulation: A
420 Quantitative Perspective. *Annu Rev Genet* 51:385-411.
421 16. Shu J, Chen C, Li C, & Cui Y (2020) The complexity of PRC2 catalysts CLF and SWN in
422 plants. *Biochem Soc Trans* 48(6):2779-2789.
423 17. De Vleesschauwer D*, et al.* (2018) Target of rapamycin signaling orchestrates growth-
424 defense trade-offs in plants. *New Phytol* 217(1):305-319.
425 18. Charron JB, He H, Elling AA, & Deng XW (2009) Dynamic landscapes of four histone
426 modifications during deetiolation in Arabidopsis. *Plant Cell* 21(12):3732-3748.
427 19. Pfeiffer A*, et al.* (2016) Integration of light and metabolic signals for stem cell
428 activation at the shoot apical meristem. *eLife* 5:e17023.

429 20. Leicher R, *et al.* (2020) Single-molecule and in silico dissection of the interaction
430 between Polycomb repressive complex 2 and chromatin. *Proc Natl Acad Sci U S A*
431 117(48):30465-30475.
432 21. Huang H, Ullah F, Zhou DX, Yi M, & Zhao Y (2019) Mechanisms of ROS Regulation of
433 Plant Development and Stress Responses. *Front Plant Sci* 10:800.
434 22. Li C, *et al.* (2016) Concerted genomic targeting of H3K27 demethylase REF6 and
435 chromatin-remodeling ATPase BRM in Arabidopsis. *Nat Genet* 48(6):687-693.
436 23. Han SK, *et al.* (2012) The SWI2/SNF2 chromatin remodeling ATPase BRAHMA
437 represses abscisic acid responses in the absence of the stress stimulus in Arabidopsis.
438 *Plant Cell* 24(12):4892-4906.
439 24. Wang P, *et al.* (2018) Reciprocal Regulation of the TOR Kinase and ABA Receptor
440 Balances Plant Growth and Stress Response. *Mol Cell* 69(1):100-112 e106.
441 25. Peirats-Llobet M, *et al.* (2016) A Direct Link between Abscisic Acid Sensing and the
442 Chromatin-Remodeling ATPase BRAHMA via Core ABA Signaling Pathway
443 Components. *Mol Plant* 9(1):136-147.
444 26. Van Leene J, *et al.* (2019) Capturing the phosphorylation and protein interaction
445 landscape of the plant TOR kinase. *Nat Plants* 5(3):316-327.
446 27. Scarpin MR, Leiboff S, & Brunkard JO (2020) Parallel global profiling of plant TOR
447 dynamics reveals a conserved role for LARP1 in protein translation.
448 *bioRxiv*:2020.2005.2013.094508.
449 28. Groth M, *et al.* (2016) MTHFD1 controls DNA methylation in Arabidopsis. *Nature*
450 *Communications* 7.
451 29. Gu X, *et al.* (2017) SAMTOR is an S-adenosylmethionine sensor for the mTORC1
452 pathway. *Science* 358(6364):813-818.
453 30. Ben-Sahra I, Hoxhaj G, Ricoult SJH, Asara JM, & Manning BD (2016) mTORC1 induces
454 purine synthesis through control of the mitochondrial tetrahydrofolate cycle. *Science*
455 351(6274):728-733.
456 31. Lawrence M, *et al.* (2013) Software for computing and annotating genomic ranges.
457 *PLoS Comput Biol* 9(8):e1003118.
458 32. Batzenschlager M, *et al.* (2015) Arabidopsis MZT1 homologs GIP1 and GIP2 are
459 essential for centromere architecture. *Proc Natl Acad Sci U S A* 112(28):8656-8660.
460

461

462 **Figure and figure legend**

463

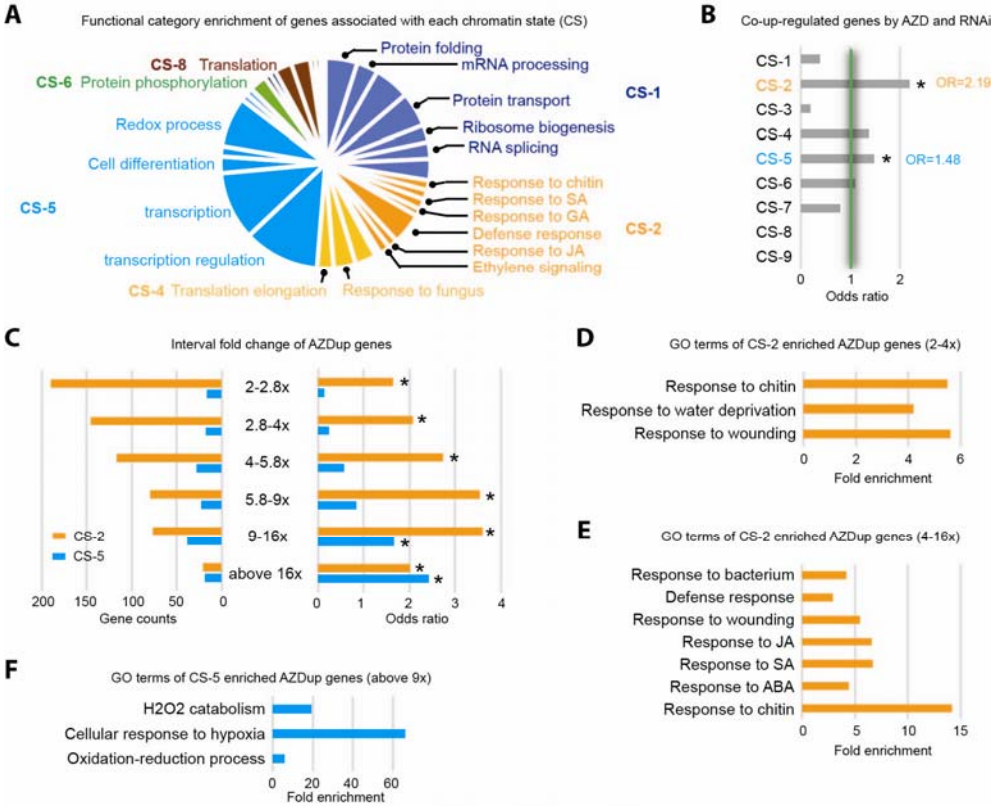

464

465

466 **Fig. 1: CS-2 and -5 specify the functional groups of TOR-responsive genes.**

467 (A) functional category analysis of genes from each chromatin state (CS) ($p<0.01$, FDR<0.1).
468 Size of pie chart indicates the relative gene number in each category. (B) Enrichment of co-
469 up-regulated genes by both AZD8055 and TOR RNAi in different chromatin states (CS; *,
470 odds ratio>1 and $p<0.05$). Different chromatin states were defined by Sequeira-Mendes *et*
471 *al*., 2014. (C) Enrichment and gene counts of different interval fold-change of up-regulated
472 genes by AZD8055 (AZDup) in CS-2 and CS-5 (*, odds ratio>1 and $p<0.05$). (D-F) Functional
473 category analysis of AZDup CS-2 genes with 2-4 fold, 4-16 fold and CS-5 genes up-regulated
474 at least 9 fold ($p<0.01$, FDR<0.1).

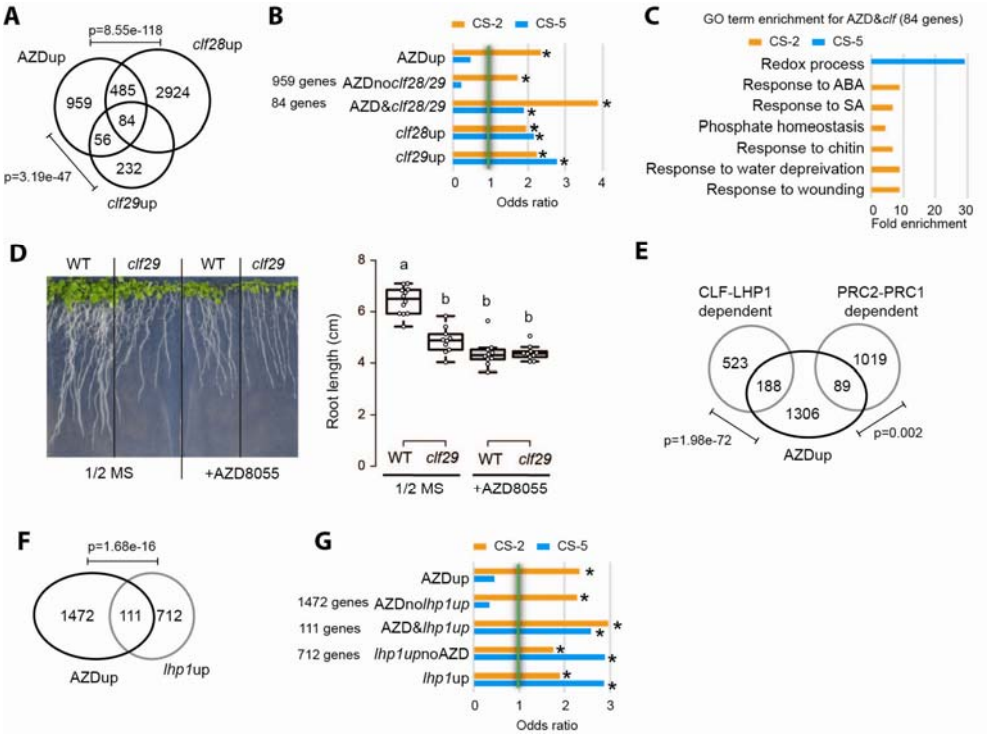

Fig. 2: TOR represses both CS-2 and 5 genes via CLF in specific context with LHP1.

(A) overlap of up-regulated genes by AZD8055 (AZDup), in *clf28* mutant (*clf28*up, hypergeometric test) and in *clf29* mutant (*clf29*up2x, hypergeometric test). (B) Enrichment of genes from different intersection between AZDup, *clf28*up and *clf29*up presented in (A) (*, OR>1 and p<0.05). (C) Functional category analysis of co-up-regulated genes by AZD8055 and in *clf28/29* enriched in CS-2 and CS-5 (p<0.01, FDR<0.1). (D) WT and *clf29* were germinated and grown on ½ MS medium or ½ MS supplemented with 0.2 µM AZD for 10 days. Bar, 1.5 cm. Root length was determined (n>10, one-way ANOVA, different letters indicated significant difference, p<0.05). (E) overlap of up-regulated genes by AZD8055 (AZDup) and context-dependent CLF regulated genes (hypergeometric test). (F) overlap of up-regulated genes by AZD8055 (AZDup) and in lhp1 mutant (*lhp1*up) (hypergeometric test). (G) Enrichment of genes from different intersection between AZDup and *lhp1*up presented in (F) (*, OR>1 and p<0.05).

490

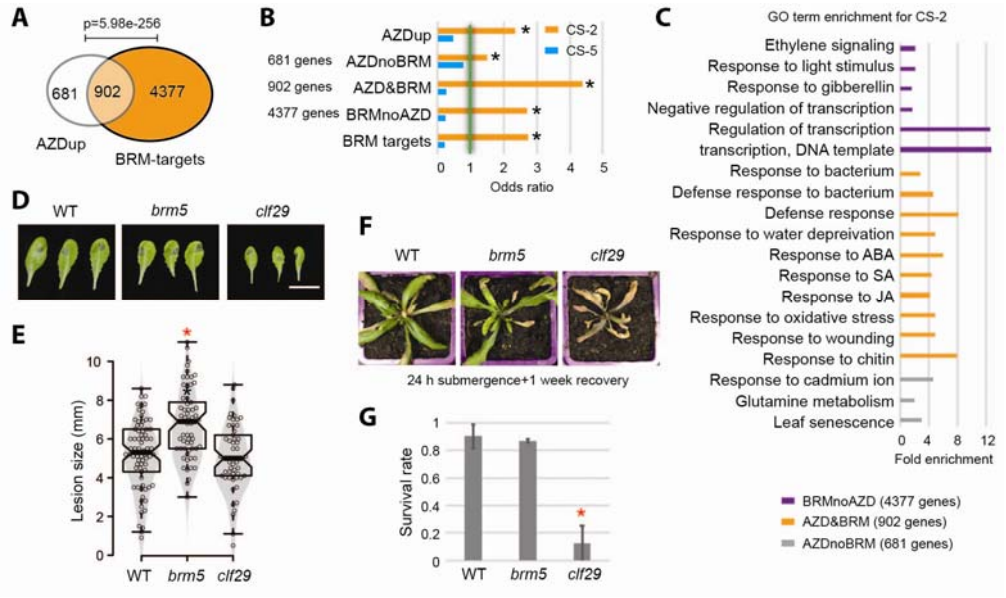

491

492

493 **Fig. 3: BRM specifically activates CS-2 genes to induce biotic stress response upon TOR**

494 **inhibition.**

495 (A) overlap of up-regulated genes by AZD8055 (AZDup) and BRM target genes

496 (hypergeometric test). (B) Enrichment of genes from different intersection between AZDup

497 and BRM targets presented in (A) (*, OR>1 and p<0.05). (C) Functional category analysis of

498 CS-2 enriched AZDup genes and BRM targets presented in (B) (p<0.01, FDR<0.1). (D) leaf

499 phenotype and (E) lesion size of *brm5* and *clf29* mutants infected by *B. cinerea* compared to

500 col-0 (n>50, central bars of the notched box represent the median, notches indicate 95%

501 confidential interval, *, p<0.05, One-way ANOVA). (F) growth phenotype and (G) survival

502 rate of *brm5* and *clf29* mutants challenged by 24 hours submergence and recovered for

503 another week (n=3, mean±s.d., *, p<0.05, One-way ANOVA).

504

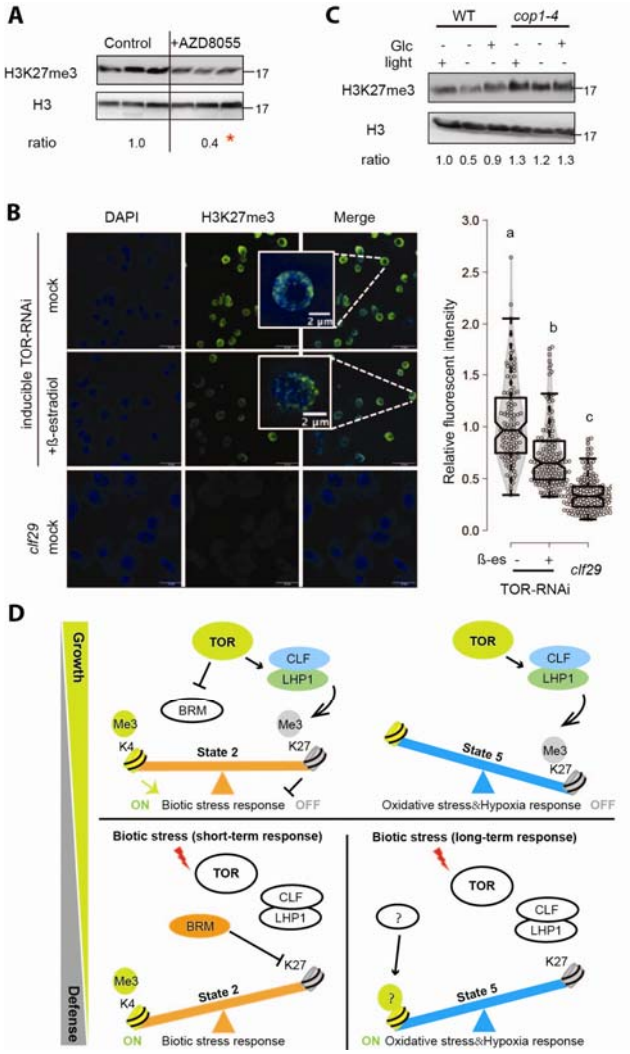

505

506

507 **Fig. 4: TOR coordinates global H3K27me3 level at different growth and developmental**

508 **stages.**

509 (A) H3K27me3 level was determined in Arabidopsis leaves treated with 1 µM AZD8055 for 24

510 hours (n=3, t-test, *, p<0.05). (B) Immuno-staining of H3K27me3 in ß-estradiol inducible

511 TOR-RNAi line and *clf29* mutant. Relative fluorescent signal was normalized against DAPI

512 signal (notches indicate 95% confidential interval, letters indicating statistic difference, One-

513 Way ANOVA, p<0.05). (C) WT and *cop1* mutant were grown under different conditions for 4

514 days. H3K27me3 and H3 level were determined by western blot. (D) Proposed model of TOR

515 function in controlling gene expression to trade-off growth and defense. We propose the

516 following scenario: active TOR up-regulates CLF and LHP1 to deposit the repressive mark
517 H3K27me3 in the bistable chromatin state 2 (CS2) and the Polycomb-associated chromatin
518 state 5 (CS5). TOR inactivation under biotic stress conditions restores the active CS2 state by
519 BRM that removes the repressive epigenetic mark to finetune the rapid biotic stress
520 response. After long-term exposure to biotic stress, plants gradually activate CS5 genes
521 involved in redox process which is more associated with a general stress response.